Origin of unit alignment in superdeformed bands in $A \approx 190$ nuclei

P. Fallon,[1] P-H. Heenen,[2] W. Satuła,[3,4,5] R. M. Clark,[1] F. S. Stephens,[1] M. A. Deleplanque,[1] R. M. Diamond,[1] I. Y. Lee,[1] A. O. Macchiavelli,[1] and K. Vetter[1]

[1]*Nuclear Science Division, Lawrence Berkeley Laboratory, Berkeley, California 94720*

[2]*Service de Physique Nucleaire Theorique, U.L.B.-C.P.229, B-105020 Brussels, Belgium*

[3]*Department of Physics, University of Tennessee, Knoxville, Tennessee 37996*

[4]*Joint Institute for Heavy-Ion Research, Oak Ridge, Tennessee 37831*

[5]*Institute for Theoretical Physics, Warsaw University, ul. Hoża 69, PL-00681 Warsaw, Poland*

(Received 29 March 1999; published 26 August 1999)

The results of an experimental and theoretical study of the inertias and alignments of superdeformed bands (SD) in $A \sim 190$ nuclei are presented. We show that $A \sim 190$ SD bands tend to be distributed among three groups characterized by their alignments and the number of unpaired nucleons. The alignments cluster around integer values ($i \approx -1,0,1$, relative to the reference chosen for this study), but the distribution is not strongly peaked: rather it is relatively ''broad'' compared with the separation, suggesting that the ''strict'' quantized alignments observed in some nuclei are not a systematic feature of all $A \sim 190$ SD bands. We further show that mean-field calculations reproduce the general experimental properties and give the three band groups seen in experiment, but they do not generally reproduce the specific alignment of SD band pairs; nor, in general, do they give ''good'' identical bands. [S0556-2813(99)03909-6]

PACS number(s): 21.10.Re, 21.60.Ev, 21.60.Jz, 27.80.+w

I. INTRODUCTION

It has been almost a decade since a superdeformed (SD) band in ^{151}Tb was found [1,2] to have the same gamma-ray transition energies (within 1–2 keV) as a superdeformed band in ^{152}Dy. Shortly after this initial discovery the first identical bands were observed [3,4] in the $A \sim 190$ region, and since then many examples have been reported in both superdeformed and normal deformed nuclei (see the recent review article [5]). The physics behind this phenomenon has stimulated much discussion, but its origin remains an open question; for example, does the occurrence of identical bands require new physics, or, as others have suggested, do they arise due to a series of ''accidental cancellations'' that lead to bands possessing the same moments of inertia and in some cases the same (identical) transition energies.

In the $A \sim 190$ region pair correlations play an important role in determining the properties of SD bands and therefore may be expected to influence the occurrence of identical bands. Indeed, the increase in the dynamic moments of inertia ($\mathfrak{I}^{(2)}$) as a function of increasing rotational frequency observed in almost all SD bands in this region is due to the occurrence of two strongly interacting *paired* band crossings involving the successive alignment of neutron (ν) and proton (π) high-j intruder orbitals [6,7]. The observed $\mathfrak{I}^{(2)}$ moments of inertia depend on the interaction strength associated with the band crossing and their magnitudes are clearly sensitive to the pairing strength. Since pair correlations are affected (reduced) by the presence of unpaired (odd) particles near the Fermi level, it is not obvious why the $\mathfrak{I}^{(2)}$ moment of inertia of $A \sim 190$ SD bands in neighboring even-mass and odd-mass nuclei should be so similar, let alone why some of these nuclei may also display identical transition energies over many (~ 10) transitions.

There are, nevertheless, several properties of $A \sim 190$ SD bands which lead to moments of inertia that are more similar than one may have first thought. (1) The Fermi level lies at or near to the SD shell gaps at $Z = 80$ and 82, and $N = 112$; these gaps occur at the same deformation, which makes the shell correction term favor SD bands with similar deformations. (2) There are several high-K orbitals near the Fermi surface; these orbitals are involved in many SD band configurations and, because they are relatively insensitive to the Coriolis interaction, their quasiparticle contribution to $\mathfrak{I}^{(2)}$ is small. (3) The presence of pair correlations results in a ''smearing'' of the occupation probabilities across different high-j intruder levels, leading to more bands possessing similar intruder content and hence similar $\mathfrak{I}^{(2)}$'s. This last point should be contrasted with the situation in the $A = 150$ region where the different (characteristic) alignment properties of the valence intruder orbitals have a large effect on the $\mathfrak{I}^{(2)}$ moment of inertia. A study of the $\mathfrak{I}^{(2)}$ moments of inertia for $A = 130$, 150, and 190 SD bands, as well as a comparison with those of normal deformed bands, is given in Ref. [8], where the role of intruder orbitals and the effects of pairing are discussed. More recently, a systematic study of identical bands was presented in Ref. [9].

In addition to identical moments of inertia, bands that also possess identical transition energies must have ''quantized'' alignments[1] simply because the level spins themselves are quantized. The alignment (i) is the difference in spin, with respect to a chosen reference band, at a fixed rotational frequency. The surprise in the mass-190 region was that gamma

[1]When comparing bands in even mass nuclei or bands in odd mass nuclei, quantized refers to $i = 0,1,2,\ldots,\hbar$, etc. Comparing a band in an even mass nucleus with one in an odd-mass nucleus requires 1/2 integer alignment to give transitions of the same energy.

rays with the same transition energies did not always appear to originate from levels with the same spin; i.e., the alignment was not zero, as one may have expected. It was proposed [3,4] that the SD bands ^{191}Hg(2,3), ^{193}Hg(2,3), and ^{194}Hg(2,3) had alignment $i \approx 1$, relative to ^{192}Hg(1). (Numbers in parentheses following the nucleus refer to a particular SD band.) The fact that $i \approx 1\hbar$, and not zero, was suggested as evidence for pseudospin alignment, a phenomenon where the (pseudo)intrinsic spins $\tilde{s}$ of the nucleons decouple from the (pseudo)orbital angular momentum $\tilde{l}$ and under the action of the Coriolis force align with the rotation axis to give the extra one unit of spin, $i = 2\tilde{s} = 1$. However, because the level spins had not been measured, an extrapolation (spin-fit) procedure [10,11] was used to determine the spins of the superdeformed states, and consequently the occurrence of unit alignment was controversial. The observation of SD bands in ^{191}Au [12], which have $1/2\hbar$ alignment with respect to ^{192}Hg, has been suggested as evidence for the odd quasiproton occupying one level of the pseudospin doublet, $i = \tilde{s} = 1/2$. Moreover, the identical SD bands observed in ^{152}Dy and ^{151}Tb [1,2] were cited as evidence for the validity of the pseudospin coupling scheme because the resulting pseudo Nilsson asymptotic quantum numbers, rather than the usual Nilsson asymptotic quantum numbers, gave the observed value of the decoupling parameter, $a = 1$. The relationship between the decoupling parameter and the pseudospin coupling scheme is discussed in Ref. [13].

Recently, gamma-ray decays from superdeformed to low-lying normal deformed states have been observed in ^{194}Hg(1,3) [14,15] and ^{194}Pb(1) [16,17], enabling the level spins in these SD nuclei to be unambiguously determined. It was shown that ^{194}Hg band 3 has odd integer spins in agreement with the spin-fit procedure, thus confirming the unit alignment proposed by Stephens *et al.* [3,4]. However, while unit alignment is confirmed, these data on the decay of the excited SD band ^{194}Hg(3), both to the normal deformed states and the yrast (ground state) SD band ^{194}Hg(1), suggest that ^{194}Hg(3) has negative parity unlike its identical band partner, ^{192}Hg, which most likely has positive parity. An observed parity difference between identical bands would rule out pseudospin alignment as the mechanism responsible for generating the observed unit alignment, since pseudospin partners have the same parity.

This paper presents the results of an experimental and theoretical study of the inertias and alignments of superdeformed bands in $A \sim 190$ nuclei to determine to what extent the experimental properties (e.g., unit alignment) can be described by present calculations. In Secs. II and III we present the results from studies of experimental data and calculation, respectively, and show that SD bands around $A = 190$ can be grouped into three families according to whether the bands have (i) a zero-quasiparticle structure, (ii) at least one neutron or one proton quasiparticle, or (iii) both neutron and proton quasiparticles. We find that theory reproduces the occurrence of three groups of SD bands, but does not give identical band pairs to the same degree as seen in experiment. In Sec. IV the results of detailed microscopic calculations are used to suggest an understanding of the observed

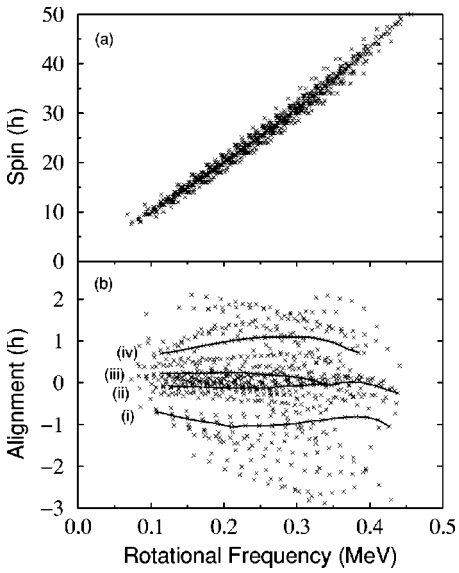

FIG. 1. (a) The level spins of SD bands in the $A \sim 190$ region plotted as a function of rotational frequency ($\hbar\omega = E_\gamma/2$). The level spins were obtained using a spin-fit procedure. (b) Alignment of the bands in (a) obtained by subtracting a reference derived from a third-order polynomial fit to all the data points: $I(E_\gamma) = a + bE_\gamma + cE_\gamma^2 + dE_\gamma^3$, where $a = 0.95$, $b = 0.04498$, $c = 3.761 \times 10^{-6}$, and $d = 7.227 \times 10^{-9}$. The solid lines (i), (ii), (iii), and (iv) correspond to the following SD bands: ^{192}Hg(1), ^{193}Hg(2), ^{193}Tl(1), and ^{194}Tl(1), respectively.

near unit alignments. These calculations indicate that both valence quasiparticles and the ''core'' contribute to these alignments and hence they do not have a unique source.

II. STUDY OF EXPERIMENTAL ALIGNMENTS AND INERTIAS

The results from a ''global'' study of $A \sim 190$ SD band alignments and moments of inertia are presented in this section. We show that the relative spins (alignments) are not ''randomly'' distributed, but they tend to lie within one of three groups characterized by their alignment and depending on their quasiparticle structure. It is further shown that these alignments are of the order of $\sim 1\hbar$ and result from low-spin effects.

A plot of spin (I) versus rotational frequency ($\hbar\omega = E_\gamma/2$) for 57 $A \sim 190$ SD bands is shown in Fig. 1(a) illustrating the similarity of $A \sim 190$ SD bands to each other. The data (transition energies) were taken from the table of superdeformed nuclear bands and fission isomers [18]. On closer inspection, however, there are differences between the bands that can be seen more clearly [Fig. 1(b)] after a reference curve (band) has been subtracted. Figure 1(b) represents the alignment, $\Delta I = I_{\rm band} - I_{\rm ref}$ (obtained at the same frequency), where $I_{\rm band}$ is the spin of a known band and $I_{\rm ref}$ is the spin of the reference band. This reference was defined to be the ''average'' band obtained by fitting a third-order polynomial to all the data points, and the alignment for each band was

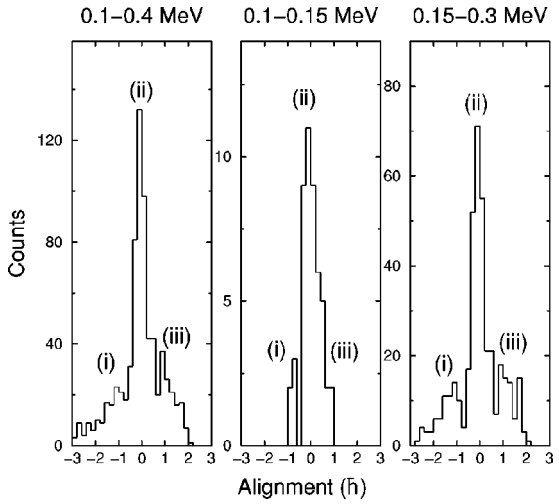

FIG. 2. The projection of the data points in Fig. 1(b) onto the spin axis. Since a reference has been subtracted (as described in the caption to Fig. 1), this plot gives the alignment (spin difference at a fixed rotational frequency) relative to the reference ''band'' (defined in the text). The left-hand plot contains data over the entire frequency range ($\hbar\omega$~0.1–0.4 MeV), the center plot is restricted to the frequency range $\hbar\omega$=0.1–0.15 MeV, and the right-hand plot has data restricted to $\hbar\omega$=0.15–0.3 MeV. The restricted frequency ranges were chosen to correspond to be either (a) just below the point or (b) in the range where the separation in spin (alignment) is most pronounced in Fig. 1(b). The labels refer to the majority-band-type contributing to each of the three distributions, i.e., (i) even-even zero-quasiparticle (SD ground state) bands, (ii) singly blocked bands with either an unpaired proton or neutron, or (iii) doubly blocked bands corresponding to the occupation of both an unpaired proton and neutron orbital (a two-quasiparticle state).

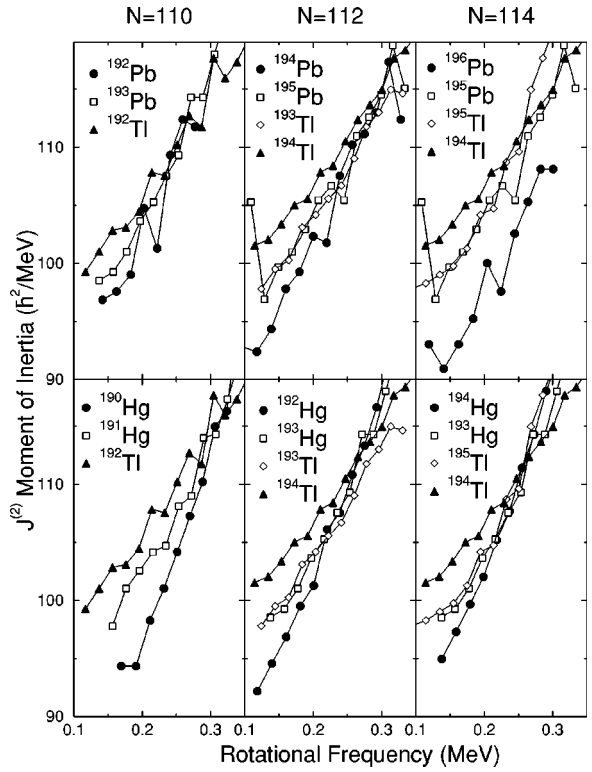

FIG. 3. The dynamic moments of inertia, $\mathfrak{I}^{(2)}$, as a function of the rotational frequency for selected $A\sim 190$ SD bands. Each plot contains four (or three) SD bands consisting of an even-even zero-quasiparticle ''core,'' neighboring singly blocked bands, and a doubly blocked band. Singly blocked refers to the occupation of an unpaired proton or neutron orbital (a one-quasiparticle state) and doubly blocked refers to the occupation of both an unpaired proton and neutron orbital (a two-quasiparticle state). Note that in all cases the blocked configuration does not involve a high-j neutron intruder (see text for details). The inertias deviate at the lowest frequencies and then become similar at higher frequencies. The neutron numbers at the top refer to the even-even (core) nucleus in that column. The following bands were used: ^{190}Hg(1), ^{191}Hg(2), ^{192}Hg(1), ^{193}Hg(2), ^{194}Hg(1), ^{192}Tl(3), ^{193}Tl(1), ^{194}Tl(1), ^{195}Tl(1), ^{192}Pb(1), ^{193}Pb(5), ^{194}Pb(1), ^{195}Pb(3), and ^{196}Pb(1). Numbers in parentheses refer to the particular band.

calculated at the rotational frequency corresponding to the observed gamma-ray transition. Recall that the spins for most SD bands have not been measured and a spin-fit procedure was used to determine the level spins.

Between $\hbar\omega$=0.15 and 0.3 MeV the data points (i.e., bands) separate into three groups, suggesting the occurrence of three ''families'' of SD bands offset in spin with respect to each other. These three groups are seen more clearly by projecting the $\Delta I-E_\gamma$ plot [Fig. 1(b)] onto the spin axis, as shown in Fig. 2. The projection was carried out over the full rotational frequency range spanned by the SD bands, $\hbar\omega$ =0.1–0.4 MeV, and over the restricted ranges $\hbar\omega$=0.1–0.15 MeV and $\hbar\omega$=0.15–0.30 MeV. The restricted frequency ranges were chosen to correspond to be either (a) just below the point or (b) in the range where the separation in spin (alignment) is most pronounced in Fig. 1(b). Since the plots in Fig. 2 are projections, each band contributes several alignment values. The three ''peaks,'' which correspond to the three groups, are separated by $\sim 1\hbar$, but the peaks are not narrow (not ''delta functions''); instead they are broad relative to the $\sim 1\hbar$ separation. Most bands have $i\approx 0$ relative to our reference.

Another way to view the separation of the SD bands into the three groups is to compare the moment of inertia, $\mathfrak{I}^{(2)}$, for neighboring SD bands at low rotational frequency.[2] Each plot in Fig. 3 contains an even-even yrast SD band (the ''core'') together with SD bands from neighboring nuclei with either an odd neutron or proton, or both an odd neutron and an odd proton: e.g., the lower middle plot in Fig. 3 shows the $\mathfrak{I}^{(2)}$ for $^{192}_{80}$Hg$_{112}$(1), $^{193}_{80}$Hg$_{113}$(2), $^{193}_{81}$Tl$_{112}$(1), and $^{194}_{81}$Tl$_{113}$(1). The band ^{193}Hg(2) was used rather that ^{193}Hg(1) since the latter interacts [20] with (crosses) another

[2]Superdeformed bands with an unpaired intruder orbital are not included in Fig. 3 because the occupation of a single (unpaired) intruder orbital ''blocks'' the paired band crossing leading to a ''flat'' $\mathfrak{I}^{(2)}$ moment of inertia [19] and hence these bands have very different alignments with respect to those bands with an even number of intruder orbitals occupied.

SD band, ^{193}Hg(4), thereby introducing large irregularities that obscure the phenomenon we wish to study. We will refer to these plots as $\mathcal{I}^{(2)}$ sets. The three families, evident in the aligned spin plot (Fig. 2), are clearly seen for each $\mathcal{I}^{(2)}$ set. Without exception, at low frequency, the yrast even-even bands have the lowest $\mathcal{I}^{(2)}$, the neighboring even-odd/odd-even singly odd (π or ν) bands have a larger $\mathcal{I}^{(2)}$, and the doubly odd bands (π and ν) have the largest $\mathcal{I}^{(2)}$ values. As the rotational frequency increases, the $\mathcal{I}^{(2)}$ curves become similar, and between $\hbar\omega \approx 0.25$ and 0.35 MeV they are very similar irrespective of whether the band is even-even, even-odd/odd-even, or odd-odd.

The low-spin deviations in $\mathcal{I}^{(2)}$ (and the corresponding alignments) are also found to be largely independent of (i) the number of *like* quasiparticles outside the even-even core nucleus (e.g., the one-quasineutron bands in ^{193}Hg have the same $\mathcal{I}^{(2)}$ as the two-quasineutron bands in ^{194}Hg), and (ii) whether the odd particle is a proton or a neutron [e.g., ^{193}Hg(2) has the same $\mathcal{I}^{(2)}$ as ^{193}Tl(1) at low frequencies]. The ''average-band'' reference used in this study has the alignment properties of a ''singly odd'' band, but is also the same as that of the two-quasineutron SD bands in ^{194}Hg (bands 2 and 3), thus further emphasizing the point that the alignments do not depend on whether one or two quasineutrons are involved, as long as the intruder state is not blocked.

The separation between the $\mathcal{I}^{(2)}$ curves in Fig. 3 suggests a simple correlation between the group to which each band belongs and the number of quasiparticles (unpaired nucleons) associated with that band. We find that $A \sim 190$ SD bands are grouped according to whether they contain (i) no unpaired particles (i.e., a zero-quasiparticle ground-state band in an even-even nucleus), (ii) either unpaired neutrons *or* protons (e.g., a one-quasiparticle band in an even-odd/odd-even nucleus), or (iii) both unpaired neutrons *and* protons (e.g., a two-quasiparticle band in an odd-odd nucleus). That is, it is only necessary to consider whether the number of unpaired quasiparticles, either neutron or proton, is zero or nonzero. This simple approach correctly places ~80% of the SD bands used in Fig. 1 as even-even, even-odd/odd-even, or odd-odd. Excluding bands that are believed to have an odd number of occupied neutron intruder orbitals results in over 90% of the SD bands being correctly identified. The solid lines in Fig. 1(b), labeled (i), (ii), (iii), and (iv), correspond to the SD bands ^{192}Hg(1), ^{193}Hg(2), ^{193}Tl(1), and ^{194}Tl(1), which are examples of even-even, even-odd, odd-even, and odd-odd bands, respectively.

The occurrence of three groups of bands [Figs. 1(b), 2, and 3] requires two things to happen. First, at low spins (low rotational frequency $\hbar\omega$), $\mathcal{I}^{(2)}$ deviates, resulting in a nonzero alignment between SD bands in different groups. Second, at some rotational frequency (which turns out to be $\hbar\omega \sim 0.25$ MeV in the experimental data), the $\mathcal{I}^{(2)}$ values must become similar and remain so for many transitions. The frequency at which the $\mathcal{I}^{(2)}$ moments of inertia become similar defines the alignment for those bands ($i = \Delta I = \int_0^{\omega} \Delta\mathcal{I}^{(2)} d\omega$)—it is important to note that if the moments of inertia continued to deviate one would not observe distinct (separate) peaks in the alignment plot (Fig. 2).

From these observations a number of questions come to mind. Why do the bands deviate at low frequency? Why is $\mathcal{I}^{(2)}$ so similar at higher frequencies? Why is the alignment $\sim 1\hbar$? Probably the simplest qualitative explanation for the low-spin deviations is that they arise due to the effects of ''pair blocking.'' Pair correlations ''suppress'' the generation of angular momentum and lead to a smaller moment of inertia than the unpaired value. In this picture, the even-even fully paired state has the lowest $\mathcal{I}^{(2)}$. Adding a neutron or proton into a state near the Fermi surface removes that state from the correlation, thus reducing the magnitude of the pairing strength and resulting in an increased moment of inertia. Similarly, blocking both a neutron and a proton orbital has a greater effect and the moment of inertia is larger still. This is precisely the feature observed in experiment and thus, at least qualitatively, the pair-blocking scenario is in agreement with the data. The differences in the moments of inertia due to pair blocking result in a change in alignment of many nucleons; it is the difference in the ''core'' alignment, not that of the odd quasiparticle itself, which generates the extra spin (of course it is the presence of the odd quasiparticle that causes the core to be different in the first place).

In Ref. [21] the effect on the pairing strength due to blocked quasiparticle levels was investigated in $A \sim 190$ SD bands. It was shown that after one neutron or proton orbital is blocked the already reduced static pair gap is practically quenched, leaving only the so-called dynamical pairing. Therefore the addition of further neutrons (protons) does not greatly alter the strength of the pair correlations. The effect of reduced pair correlations on the moments of inertia, due to blocking, was investigated further in Ref. [22] where improved quantitative agreement with experiment was achieved by including both seniority and quadrupole pairing interactions.

While pair blocking provides a plausible (qualitative) explanation for the observed differences in the moments of inertia (i.e., why the bands deviate at low spin) the observed alignments could have their origin in a number of effects, i.e., $\Delta I = \delta i_{\mathrm{qp}} + \delta i_{\mathrm{pairing}} + \delta i_{\mathrm{def}} + \ldots$, where δi_{qp} is the contribution to the alignment from the valence particle(s), $\delta i_{\mathrm{pairing}}$ is due to the ''quenching'' of pairing, and δi_{def} is the effect due to changes in deformation. (The decomposition into various contributions is somewhat arbitrary, and it is recognized that the terms given above are not necessarily independent.) In previous works the alignment between SD bands has been mainly discussed in terms of the contribution from δi_{qp}. The pseudospin alignment explanation [3,4] for unit alignment in identical bands and the study of the alignments in Tl isotopes relative to ^{192}Hg [23] are both examples where the valence quasiparticles are considered to provide the dominant contribution. Whether the origin of the $\mathcal{I}^{(2)}$ differences in $A \sim 190$ SD bands at low rotational frequency is pair blocking and/or quasiparticle alignment, it is clear that they need to become sufficiently small at higher frequencies so that bands in neighboring nuclei exhibit very similar moments of inertia over many transitions.

III. CALCULATED PROPERTIES

In order to gain insight into the relative contributions to the total alignment (i.e., quasiparticle and/or core-pairing effects) we performed a study of calculated $A\sim 190$ SD bands comparable to that carried out for experimental data. Section III A contains a brief description of the calculations, and Section III B contains the results from a systematic study of the calculated bands and a comparison with experiment.

A. Theoretical models

There are already a number of published applications of the Strutinsky method [24,25] as well as fully self-consistent Hartree-Fock-Bogoliubov (HFB) calculations involving both Skyrme [26,27] and Gogny [28,29] interactions. In all these works the inclusion of higher order pairing effects and the restoration of good particle number was found to be necessary to assure proper treatment of $A\sim 190$ SD bands. In fact, techniques such as the double-stretched quadrupole pairing interaction [25], the surface-active density-dependent delta interaction [30], and the Lipkin-Nogami (LN) number-projection techniques [31–35] were first applied in large-scale calculations in $A\sim 190$ SD nuclei [24–28]. Afterwards, following numerous successful applications in other mass regions, they became standard methods for high-spin physics.

Most publications addressing the physics of SD bands deal with band-to-band comparisons between theoretical and experimental data. In what follows we will compare the *relative* properties of SD bands (alignments, inertias, etc.) obtained from experiment with the same relative quantities from calculation. The aim of this work is (i) to perform large-scale calculations and make global comparisons of various calculated and measured properties for many SD bands and (ii) to look into the physical mechanisms responsible for the occurrence of certain systematic effects such as, for example, the alignments that lead to the three groups of SD bands discussed above. Two types of cranked mean-field calculations were performed: total Routhian surface (TRS) Strutinsky-type calculations and fully self-consistent Skyrme-Hartree-Fock-Bogoliubov (Skyrme-HFB) calculations. Not all the possible configurations assigned to experimental SD bands were available from calculation (especially for HFB calculations, which are more time consuming than TRS calculations) and thus only a limited data set was used to compare experiment and calculation. The configurations were chosen to be consistent with the experimental bands in Fig. 3 and are generally the most energetically favorable for each parity and signature.

The TRS calculations involve a deformed Woods-Saxon (WS) potential [36] in the particle-hole (p-h) channel, and seniority and double-stretched quadrupole pairing interactions in the particle-particle (p-p) channel. The LN approximate number-projection technique [31–35,24,26] is used to prevent the collapse of pairing at higher rotational frequencies. The strength of the seniority pairing force is calculated using the average gap method [37] and the strength of the quadrupole pairing interaction is calculated at zero frequency using the method of Ref. [38], which restores local Galilean invariance. The total Routhian is calculated using the Strutinsky shell-correction method [39,40] on a mesh in deformation space involving quadrupole (β_2 and γ) and hexadecapole (β_4) deformations. The macroscopic energy is described using the liquid-drop model of Ref. [41]. The pairing p-p channel is treated fully self-consistently; i.e., the LN equations are solved rigorously at each deformation point and at each rotational frequency. For further details on the model we refer the reader to Refs. [25, 24, 42]. It is important to stress that the parameters of both the WS potential and the strengths of the pairing force were adjusted to reproduce global properties across the nuclear chart and for a wide range of deformations, and no additional readjustments have been done to improve the agreement of TRS calculations with the present data on $A\sim 190$ SD bands.

The TRS calculations have been performed for $N=108-116$ isotones of $_{79}$Au, $_{80}$Hg, $_{81}$Tl, and $_{82}$Pb. For even-even nuclei only the vacuum configuration was calculated and for each odd (odd-odd) nucleus 4 (16) one- (two-) quasiparticle configurations were calculated. However, only a limited number of the total TRS calculated bands were used for this study. The quasiparticles occupied the lowest states of a given signature and parity (π,α) at zero rotational frequency.

The method used to perform Skyrme-HFB calculations has been presented in Ref. [27]. The nucleon-nucleon effective interaction in the particle-hole channel is the Skyrme force within the SLy4 parametrization [43]. In the pairing channel we use a zero-range force with a surface-peaked density dependence as described in Ref. [27], with the parametrization adapted to the SLy4 Skyrme force and derived in a study of SD in the mass $A=150$ region [44]. As for the TRS calculations, the mean-field method has been corrected by means of the LN prescription to take into account the finite number of nucleons. This combination of mean-field p-h and p-p (pairing) forces has been shown to lead to a good description of $\mathcal{I}^{(2)}$ values for SD bands. The quasiparticle excited bands were treated fully self-consistently as in Refs. [45,46]. The HFB calculations, being significantly more time consuming than TRS calculations, were limited to fewer configurations.

B. Dynamical moments of inertia and alignments

The calculated (TRS and HFB) $\mathcal{I}^{(2)}$ values are given in Fig. 4. The same SD bands (configurations) as shown in Fig. 3 were used, and the calculated $\mathcal{I}^{(2)}$ curves were subdivided into $\mathcal{I}^{(2)}$ sets comprising four or three SD bands. The yrast even-even bands have the lowest $\mathcal{I}^{(2)}$, the neighboring one quasiparticle even-odd/odd-even bands have larger $\mathcal{I}^{(2)}$'s, and the two quasiparticle odd-odd bands have the largest $\mathcal{I}^{(2)}$ values, in agreement with experiment although for both TRS and HFB calculations the spread in $\mathcal{I}^{(2)}$ is larger than experiment. The larger dispersion in $\mathcal{I}^{(2)}$ means there will be a correspondingly larger alignment. An additional problem arises for ^{190}Hg calculated from TRS; the $\mathcal{I}^{(2)}$ is too large at $\hbar\omega\approx 0.3$ MeV. This, as discussed in Ref. [25], is because the neutron-paired band crossing occurs too soon in the TRS calculation for $N=110$. We also note that in TRS calcula-

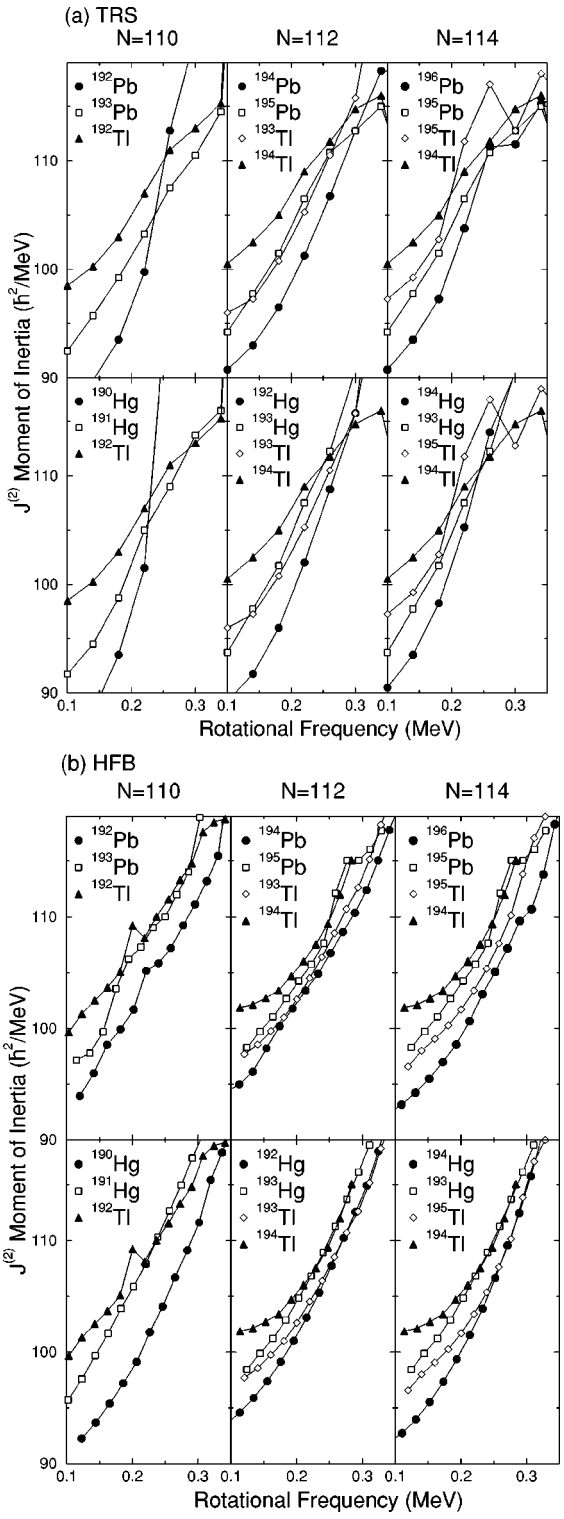

FIG. 4. Same as Fig. 3, but for calculated $A\sim 190$ SD bands. The results from (a) TRS and (b) HFB calculations are shown. The following band configurations were used: ^{190}Hg(V), ^{191}Hg(A), ^{192}Hg(V), ^{193}Hg(A), ^{194}Hg(V), ^{192}Tl($pAnA$), ^{193}Tl(A), ^{194}Tl($pBnA$), ^{195}Tl(A), ^{192}Pb(V), ^{193}Pb(A), ^{194}Pb(V), ^{195}Pb(A), and ^{196}Pb(V), where V is the vacuum configuration, p and n refer to either quasiproton or quasineutron, and A and B are the lowest $+$ parity, $+$, $-$ signatures, respectively. These configurations correspond to those assigned to the experimental bands in Fig. 3.

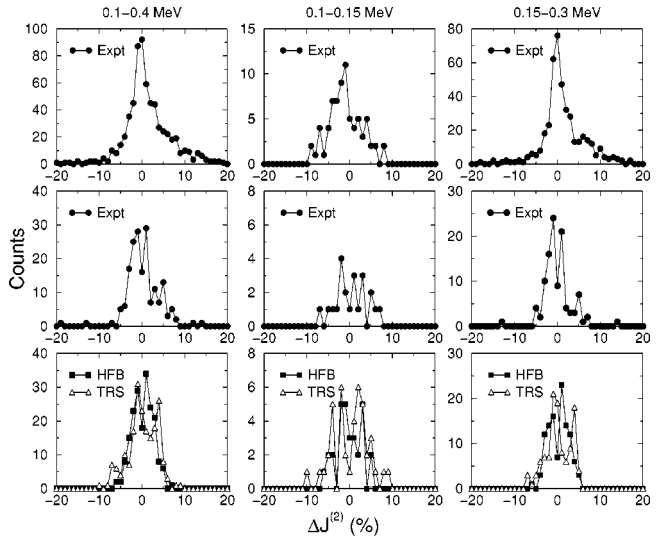

FIG. 5. Distribution of $\mathfrak{I}^{(2)}$, the variation in the dynamic moments of inertia, between $A\sim 190$ SD bands. The difference $\Delta\mathfrak{I}^{(2)}$ is given relative to the appropriate reference band for either experiment or calculation (see text for details). Solid circles are from experiment (top two rows), and solid squares and open triangles are from HFB and TRS calculations, respectively (bottom row). The top row gives the distribution for the 57 experimental SD bands considered in this study. The middle and bottom rows give the distribution for the same 14 experimental and calculated SD bands in Figs. 3 and 4, and allows a direct comparison between experiment and calculation to be made. In all cases the distribution in $\mathfrak{I}^{(2)}$ was determined over three frequency ranges: corresponding to the full range $\hbar\omega\sim$0.1–0.4 MeV (left column), $\hbar\omega$=0.1–0.15 MeV (center column), and $\hbar\omega$=0.15–0.3 MeV (right column).

tions the configuration of the minimum energy solution may change adiabatically, and as a consequence, interpolation on the lattice (mesh) may result in significant fluctuations in the calculated $\mathfrak{I}^{(2)}$, especially at higher frequencies in the vicinity of the paired band crossings. The HFB calculated $\mathfrak{I}^{(2)}$ curves show less fluctuation compared with the TRS curves, and at higher rotational frequencies there is the tendency for them to converge towards two curves rather than the single curve seen in experiment. In HFB calculations it is the bands which differ by an odd proton rather than those differing by an odd neutron that have identical $\mathfrak{I}^{(2)}$'s at higher frequencies. For example, ^{193}Tl and ^{192}Hg have the same $\mathfrak{I}^{(2)}$ for $\hbar\omega\geqslant$0.25 MeV, as do ^{194}Tl and ^{193}Hg.

The distribution of $\Delta\mathfrak{I}^{(2)}$ is shown in Fig. 5 for the experimental data and the TRS and HFB calculations. The percentage variation in $\mathfrak{I}^{(2)}$ ($\Delta\mathfrak{I}^{(2)}$) was obtained from

$$\Delta\mathfrak{I}^{(2)}=100\times\frac{\mathfrak{I}^{(2)}(\omega)-\mathfrak{I}^{(2)}_{\rm ref}(\omega)}{\mathfrak{I}^{(2)}_{\rm ref}(\omega)}.$$

The reference band is once more taken to be the *average* of either the experimental, TRS, or HFB calculated SD bands and the difference $\Delta\mathfrak{I}^{(2)}$ was obtained at several frequency intervals $\Delta\hbar\omega\approx$20 keV. The top row in Fig. 5 gives the distribution of $\Delta\mathfrak{I}^{(2)}$ for the 57 experimental SD bands considered in this study. The middle and bottom rows give the

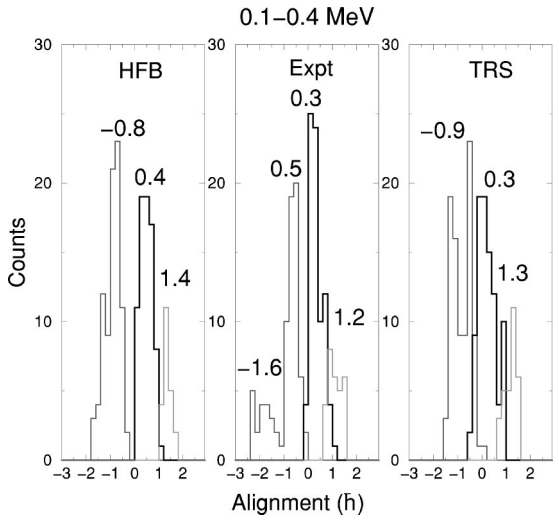

FIG. 6. Alignment of the 14 $A\sim190$ SD bands shown in Figs. 3 (experiment) and 4 (HFB and TRS calculations). For each set (experiment, HFB, TRS) the bands were compared with an average reference band derived from the 14 bands within each set. Separate histograms are shown for even-even ground-state, odd-even/even-odd ''singly'' blocked, and odd-odd two quasiparticle SD bands. In each plot the central peak (thick line) corresponds to the odd-even/even-odd ''singly'' blocked bands; the peaks to the left and right are the even-even zero quasiparticle and odd-odd two quasiparticle bands, respectively. The average alignment for each of the band types is given above each peak. In experiment the even-even bands produce two peaks at -1.6 and $0.5\hbar$.

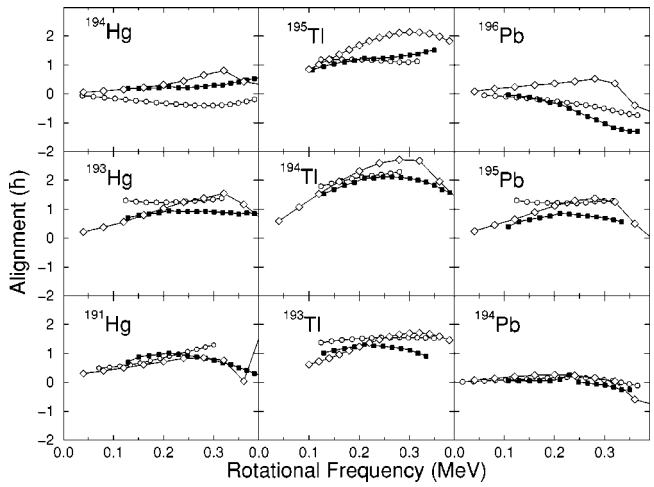

FIG. 7. Experimental (solid squares) and calculated alignments for a range of $A\sim190$ SD bands relative to that of the yrast ^{192}Hg SD band. TRS and HFB data points are given by open diamonds and open circles, respectively. Experimental alignments are relative to ^{192}Hg band 1 and calculated alignments use the appropriate (either TRS or HFB) calculated ^{192}Hg vacuum band. The following bands (and configurations) were used; ^{191}Hg band 2 (nA); ^{193}Hg band 2 (nA), ^{194}Hg band 1 (V), ^{193}Tl band 1 (pA), ^{194}Tl band 1 ($pBnA$), ^{195}Tl band 1 (pA), ^{194}Pb band 1 (V), ^{195}Pb band 3 (nA), and ^{196}Pb band 1 (V), where V is the vacuum configuration, p and n refer to either quasiproton or quasineutron, and A and B are the lowest + parity, +, − signatures, respectively.

distribution for the 14 experimental and calculated SD bands shown in Figs. 3 and 4, and since the same 14 bands (configurations) are considered, these plots allow direct comparison between experiment and calculation. In all cases the distribution in $\mathfrak{I}^{(2)}$ was determined over three frequency ranges: (i) the full range $\hbar\omega=0.1$–0.4 MeV (left column), (ii) $\hbar\omega=0.1$–0.15 MeV (center column), and (iii) $\hbar\omega=0.15$–0.3 MeV (right column). As expected, from the $\mathfrak{I}^{(2)}$ curves in Figs. 3 and 4, the distributions are wider at low frequencies and they become narrower above $\hbar\omega=0.3$ MeV. The distributions for the TRS and HFB calculations are similar (lower row of plots) and both are slightly broader than experiment (middle row).

Having shown, in Fig. 4, that the three groups of SD bands are evident in the calculated $\mathfrak{I}^{(2)}$ curves, we now consider their alignments. Figure 6 gives the alignment of HFB calculated bands together with the corresponding experimental bands. The plot was generated using the same method as Fig. 2. Each set of SD bands (experiment, HFB, TRS) was compared with its own (internal) average reference band derived from a third-order polynomial fit to the 14 bands within each set. In each plot the central peak (thick line) corresponds to the odd-even/even-odd bands and the peaks to the left and right are derived from even-even and odd-odd bands, respectively. The peaks contain the following band types: (i) Left peak: ^{190}Hg(1), ^{192}Hg(1), ^{194}Hg(1), ^{192}Pb(1), ^{194}Pb(1), ^{196}Pb(1) (even-even bands). (ii) central peak: ^{191}Hg(2), ^{193}Hg(2), ^{193}Tl(1), ^{195}Tl(1), ^{193}Pb(5), ^{195}Pb(3) (odd-even/even-odd bands). and (iii) Right peak: ^{192}Tl(3), ^{194}Tl(1) (odd-odd bands). A similar separation of the three groups (band types) is observed in all three data sets (experiment, HFB, TRS). The numerical value of the average alignment for the three groups (band types) is shown in the figure. Since more even-even SD bands were used, compared with odd-odd bands, the reference used does not give an alignment for the odd-even/even-odd bands that is centered at $i\approx0\hbar$. However, the separation between the different band types is still $\Delta i\approx1\hbar$. Note that in experiment the even-even bands are split; the ''peak'' at $i\sim-1.6\hbar$ is due to the yrast SD bands in ^{190}Hg and ^{196}Pb. These bands have the smallest $\mathfrak{I}^{(2)}$ values at low frequencies.

A quantitative comparison of experimental and calculated alignments for individual band pairs was also carried out, enabling the alignments to be studied as a function of rotational frequency on a case-by-case basis. These are plotted in Fig. 7 as a function of rotational frequency relative to ^{192}Hg(1). The yrast SD band in ^{192}Hg has typically been the reference of choice when comparing specific SD bands, and we have used this reference in Fig. 7 to allow easier comparison with previous studies. In general, both TRS and HFB calculations are able to reproduce the experimental alignments to within $\sim0.5\hbar$. While this accuracy is often sufficient when assigning specific configurations to a band it is not sufficient to resolve the question of identical bands that typically have alignments within $\sim0.1\hbar$ of an integer value for many transitions. For example, Fig. 7 indicates that calculation gives an identical band pair in at least one case (^{194}Pb-^{192}Hg) but not for every case; the ^{193}Hg signature partner bands (bands 2 and 3) based on the high-K [624]9/2

orbital are known to be very good examples of identical bands when referenced to ^{192}Hg(1), yet both the TRS and HFB calculation yield too much alignment. On the other hand, the ^{195}Tl-^{192}Hg pair provides an example where HFB calculation gives a better identical band pair than experiment. Other cases show reasonable agreement with data, at least for the HFB calculation, but for these nuclei the experimental alignment does not have an integer value over many transitions and hence they would not be considered ''good'' identical bands.

To summarize this section, we have shown that our calculations show good agreement with general experimental properties, but the calculations do not reproduce the specific alignment of SD band pairs; nor, in general, do they give ''good'' identical bands.

IV. MICROSCOPIC ORIGIN OF THE LOW-SPIN ALIGNMENTS WITHIN THE MEAN-FIELD THEORY

In this section we address the more specific question regarding the microscopic origin of the low-spin alignment; namely, is ΔI mostly due to a quenching of the bulk pairing properties (a core effect), or is it due to valence quasiparticle alignment? A basic difficulty in determining the relative roles of the ''core'' and valence quasiparticle alignments, within a mean-field theory, is that the mean field lacks the notion of a core and additional problems arise due to nuclear self-consistency, which strongly couples the pairing and shape degrees of freedom. Consequently, the conclusions given below, regarding the numerical values of the decomposition into quasiparticle ($\delta I_{\rm qp}$) and core ($\delta I_{\rm core}$) alignments, depend upon the following definitions.

In HFB theory the one-quasiparticle density matrix can be written as (see, for example, [47])

$$\rho^{(K)}_{\alpha,\beta}=\rho^{(o)}_{\alpha,\beta}-[V^*_{\alpha,K}V_{\beta,K}-U_{\alpha,K}U^*_{\beta,K}]. \tag{1}$$

Indices α,β refer to the single-particle basis, capital letters (e.g., K) refer to quasiparticle states, U and V are the usual occupation probabilities, and $\rho^{(K)}_{\alpha,\beta}$ and $\rho^{(o)}_{\alpha,\beta}$ are density matrices. Since the form of the density matrix $\rho^{(o)}_{\alpha,\beta}$,

$$\rho^{(o)}_{\alpha,\beta}=\sum_L V^*_{\alpha,L}V_{\beta,L}, \tag{2}$$

is analogous to the density matrix in an even-even nucleus, it can naturally serve as a definition of the density of a *local core* in an odd-A nucleus. Exploring further this analogy we can use Eq. (1) and write the total spin in an odd-A nucleus, $I^{(K)}_x$ (K denotes a blocked quasiparticle), as the sum of the core $I^{(o)}_x$ and quasiparticle $\delta I^{(K)}$ contributions:

$$I^{(K)}_x=\mathrm{Tr}(j_x\rho^{(K)})=I^{(o)}_x+\delta I^{(K)}_x, \tag{3}$$

where

$$I^{(o)}_x\equiv\mathrm{Tr}(j_x\rho^{(o)})\equiv\sum_L\sum_{\alpha,\beta}j^{\alpha,\beta}_x V^*_{\beta,L}V_{\alpha,L} \tag{4}$$

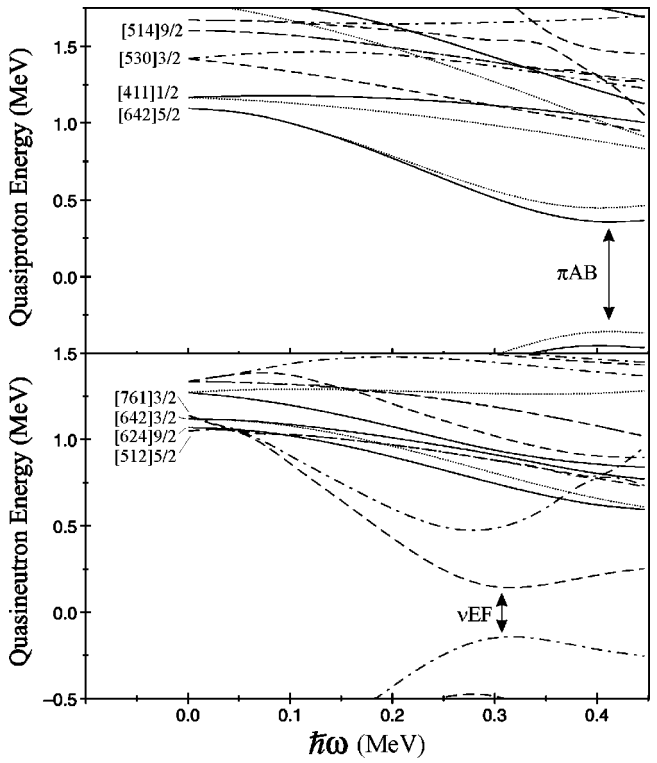

FIG. 8. Neutron and proton quasiparticle Routhians for $Z=80$, $N=112$ (^{192}Hg) at $\beta_2=0.48$, $\beta_4=0.06$, and $\gamma=0$. Asymptotic Nilsson quantum numbers label the lowest states and the parity and signature are given by (π,α): solid line$=(+,+1/2)$, dotted line$=(+,-1/2)$, dot-dashed line$=(-,+1/2)$, and dashed line$=(-,-1/2)$.

and

$$\delta I^{(K)}_x\equiv-\sum_{\alpha,\beta}j^{\alpha,\beta}_x(V^*_{\beta,K}V_{\alpha,K}-U_{\beta,K}U^*_{\alpha,K}). \tag{5}$$

Using the above and defining the spin of the even-even ''core'' nucleus as $I^{\rm core}_x$ we obtain

$$\begin{aligned}\Delta I\equiv I_x(\omega)-I^{\rm core}_x(\omega)&=[(I^{(o)}_x(\omega)-I^{\rm core}_x(\omega)]+\delta I^{(K)}_x(\omega)\\&\equiv\delta I_{\rm core}+\delta I_{\rm qp},\end{aligned} \tag{6}$$

i.e., a decomposition of the relative alignment ΔI into core and quasiparticle contributions, respectively.

Table I gives the total alignment ΔI and the contribution from quasiparticle, $\delta I_{\rm qp}$, and ''core,'' $\delta I_{\rm core}$, alignments calculated (using the HFB procedure described above) for the specified quasiparticle orbitals with respect to ^{192}Hg. To investigate only pairing properties we performed pairing self-consistent LN calculations with fixed shape parameters for the Woods-Saxon potential of $\beta_2=0.48$, $\beta_4=0.06$, and $\gamma=0$ for all nuclei listed in the table. This deformation corresponds to that of the ^{192}Hg core predicted by a TRS calculation at low rotational frequency. The decomposition, Eqs. (3)–(6), is valid for HFB calculations, but not for calculations using the LN method since this gives a prescription to recalculate observables only and not individual U and V coefficients. Therefore, for LN calculations we provided only

TABLE I. Calculated values of ΔI (in units of $\hbar$) for the lowest SD bands in $^{193}_{81}Tl_{112}$, $^{191}_{80}Hg_{111}$, and $^{193}_{80}Hg_{113}$ relative to that of the ^{192}Hg SD vacuum at two frequencies $\hbar\omega=0.08$ (i.e., near zero) and $\hbar\omega=0.28$ MeV (close to where the experimental $\mathcal{J}^{(2)}$ moments of inertia, in general, converge). Calculated quasiparticle, $\delta I_{\rm qp}$, and core, $\delta I_{\rm core}$, contributions to the alignment ΔI are compared with self-consistent Lipkin-Nogami, $\Delta I_{\rm LN}$, and TRS calculations, $\Delta I_{\rm TRS}$, and experimental data, $\Delta I_{\rm expt}$. For experiment, the alignment at $\hbar\omega=0.08$ MeV was derived by extrapolation. Calculations were performed for the lowest quasiparticle states with a given parity and signature (π,α). The quasiparticles are labeled by Nilsson quantum numbers $[Nn_z\Lambda]\Omega$ (dominant component) and by the parity and signature quantum numbers $(\pi,\alpha)=(+,+)(+,-)(-,-)(-,+)$ further abbreviated to A, B, E, and F, respectively.

	Orbital	(π,α)	$\hbar\omega$ [MeV]	$\delta I_{\rm qp}$	$\delta I_{\rm core}$	ΔI	$\Delta I_{\rm LN}$	$\Delta I_{\rm TRS}$	$\Delta I_{\rm expt}$
$Z=81$	[642]5/2	A	0.08	0.92	−0.20	0.72	0.65	0.62	0.74
			0.28	2.10	−0.44	1.66	1.53	1.50	1.43
	[642]5/2	B	0.08	0.99	−0.18	0.81	0.75	0.71	0.71
			0.28	1.82	−0.38	1.44	1.34	1.36	1.18
	[514]9/2	E	0.08	0.21	0.19	0.40	0.39	0.28	
			0.28	0.03	0.86	0.89	0.76	1.02	
	[514]9/2	F	0.08	−0.22	0.19	−0.03	−0.03	−0.06	
			0.28	−0.19	0.72	0.53	0.46	0.55	
$N=111$	[642]3/2	A	0.08	0.23	0.19	0.42	0.41	0.39	0.62
			0.28	0.01	0.96	0.97	0.85	0.84	1.03
	[642]3/2	B	0.08	0.10	0.15	0.25	0.24	0.19	0.87
			0.28	0.29	0.75	1.04	0.96	0.82	1.12
	[761]3/2	E	0.08	2.76	−0.30	2.46	2.38	2.49	2.95
			0.28	2.66	−0.05	2.61	2.55	2.85	2.69
	[761]3/2	F	0.08	1.89	−0.27	1.62	1.54	1.38	1.55
			0.28	0.68	−0.33	0.35	0.21	0.38	0.21
$N=113$	[642]9/2	A	0.08	0.18	0.24	0.42	0.42	0.37	0.55
			0.28	0.22	1.16	1.38	1.30	1.38	0.93
	[642]9/2	B	0.08	0.16	0.21	0.37	0.37	0.33	0.57
			0.28	0.29	1.15	1.44	1.35	1.46	0.97
	[752]5/2⊗[512]5/2[a]	E	0.08	0.80	0.14	0.94	0.87	1.20	0.25
			0.28	2.09	0.37	2.46	2.34	3.04	2.10
	[752]5/2⊗[512]5/2[a]	F	0.08	0.58	0.16	0.74	0.69	1.03	0.95
			0.28	0.42	0.35	0.77	0.63	0.72	0.51

[a]The $\Omega=3/2$ and 5/2 components of the $N=7$ intruder orbital ([761]3/2, [752]5/2), which originate from the spherical $j_{15/2}$ orbital, are highly mixed.

the total alignment ΔI_{LN}. The ''schematic'' results (i.e., $\delta I_{\rm qp}$, $\delta I_{\rm core}$ and ΔI) are further compared with full TRS calculations, $\Delta I_{\rm TRS}$, which include shape dynamics as a function of $\hbar\omega$ and shape changes from nucleus to nucleus. Finally, the experimental alignment $\Delta I_{\rm expt}$ is also given. The alignments presented in Table I were calculated at frequencies $\hbar\omega=0.08$ MeV and 0.28 MeV.

In almost all cases shown in Table I $\Delta I\approx\Delta I_{LN}\approx\Delta I_{\rm TRS}$, indicating relatively small corrections due to either LN renormalization of the occupation probabilities and/or details in the shape dynamics. The most important ingredients in creating ΔI are therefore pairing (core) and the quasiparticle alignments carried by a given orbital.

The relative importance of $\delta I_{\rm core}$ and $\delta I_{\rm qp}$ contributions varies from orbital to orbital. The relevant orbitals (quasiparticle Routhians) are shown in Fig. 8. The diagram is appropriate for ^{192}Hg at $\beta_2=0.465$, $\beta_4=0.048$, and $\gamma=0$. This figure also illustrates the πAB and νEF quasiparticle band crossings that give rise to the smoothly increasing $\mathcal{J}^{(2)}$.

The different alignment contributions resulting from the occupation of high-K (extruder) or low-K intruder orbitals

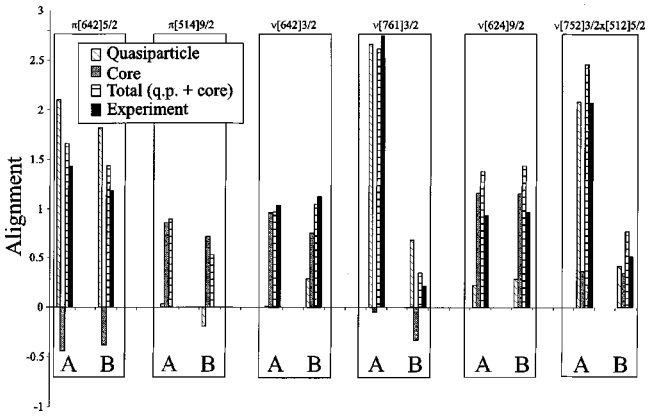

FIG. 9. Plot of the calculated alignments, at $\hbar\omega=0.28$ MeV given in Table I, due to the occupation of a single quasiproton or quasineutron level outside the ^{192}Hg core. *A* and *B* refer to the two signatures for each level. The total calculated alignment, the contribution from the valence quasiparticle, and the core are shown together with the observed experimental alignments.

are also illustrated in Fig. 9 (values are for $\hbar\omega=0.28$ MeV taken from Table I) and can be intuitively understood by considering the relative importance of the Coriolis force on these orbitals. Blocking an ''extruder'' Nilsson state, such as ν [624]9/2 or π [514]9/2, causes changes in ΔI predominantly through rearrangements in the core. The same is true, at least at higher spins, for the ν [642]3/2 state. On the other hand, for bands with the π [642]5/2 state occupied the effect is mainly due to quasiparticle alignment. Note that this orbital originates from the spherical $i_{13/2}$ intruder state. In fact, similar quasiparticlelike dominance is seen for other intruder states, e.g., ν [761]3/2 and ν [752]5/2$\otimes$[512].

In general, we find that the alignments arising from small deviations in the moments of inertia at low frequencies have both a core (pairing) and quasiparticle component. There is, nonetheless, a tendency for the relative importance of these two contributions to vary and to depend on the detailed structure, e.g., whether the odd nucleon occupies a high- or low-K orbital.

V. SUMMARY AND CONCLUDING REMARKS

The global alignment and the moment of inertia studies indicate the tendency for $A\sim 190$ SD bands to distribute themselves among the following three groups characterized by their alignments and the number of unpaired nucleons: (i) zero-quasiparticle bands, (ii) ''singly blocked'' bands with either one (or more) quasiproton(s) or quasineutron(s), or (iii) ''doubly blocked'' bands with both proton and neutron quasiparticle states. The alignments cluster around integer values ($i\approx -1,0,1$, relative to the reference chosen for this study), but the distribution is not strongly peaked: rather it is relatively ''broad'' compared with the separation, suggesting that the ''strict'' quantized alignments observed in some nuclei are not a systematic feature of all $A\sim 190$ SD bands. Both HFB and TRS (Strutinsky method) calculations reproduce these global properties and give this same distribution of bands into three groups.

For most SD bands in the $A\sim 190$ region the observed low-spin alignments are small, $\sim 1\hbar$, and several mechanisms may be expected to contribute to the effect. Indeed, the microscopic HFB calculations presented in this paper indicate that within this mean-field theory these alignments do not have a unique source. Both core and quasiparticle effects, as well as other elements such as shape changes and/or dynamical correlations, though to a lesser extent, influence the final value of the calculated alignments. There is, nonetheless, a tendency for the relative importance of the core and quasiparticle contributions to depend on the nature of the occupied quasiparticle orbital. One the one hand, the high-K neutrons around $N=112$ do not contribute a significant quasiparticle alignment and the observed alignments mainly arise due to a pair-blocking effect. Thus the expectation that the presence of an odd particle should affect pairing at low frequencies (spins), which in turn influences the generation of angular momentum, is justified by calculation. On the other hand, the near unit alignment relative to ^{192}Hg due to the occupation of the intruder [642]5/2 proton orbital (e.g., ^{193}Tl bands 1 and 2) comes mainly from the quasiparticle itself, with a smaller contribution from the core.

Let us now consider our results within the context of identical bands. In general, the calculations presented in this paper reproduce the experimental alignments to an accuracy of $\sim 0.5\hbar$. To describe the observed identical bands, however, the alignment has to be within $\sim 0.1\hbar$ of an integer value (over a wide frequency range) and thus, at this time, it is not possible for mean-field calculations to reliably reproduce the phenomenon of identical bands and provide a detailed understanding of their origin. We note, nonetheless, that the agreement with data even at the $\sim 0.5\hbar$ level is remarkable considering the complexity of the problem and that in at least one case (^{194}Pb-^{192}Hg) calculation reproduces a known identical band pair (although, as we have stressed, they do not for other cases, e.g., ^{193}Hg-^{192}Hg). While there is evidence that pseudospin likely plays a role in those identical bands that exhibit $1/2\hbar$ alignment, both in the $A\sim 150$ region (e.g., ^{151}Tb-^{152}Dy and ^{151}Dy-^{152}Dy) and in the $A=190$ region (^{191}Au-^{192}Hg), our results indicate that the occurrence of $1\hbar$ (or near $1\hbar$) alignment may be traced either to the alignment of the odd quasiparticle itself or to the influence that this quasiparticle has on the alignment of other nucleons due to the coupling through the pairing channel (i.e., core alignment). However, there is not a clean separation between quasiparticle alignment and pairing effects—both occur—and if this interpretation is correct, i.e., the alignments have in general a mixed origin, then the observed unit alignments would appear to be ''accidental.''

Finally, through the course of this paper we have attempted to answer the following questions: what is the cause of the low spin deviations in $A\sim 190$ SD bands, why is the resulting alignment $\sim 1\hbar$, and why are the moments of inertia so similar for such a long frequency range? Much progress was made in addressing these issues and valuable insight was obtained into the role of pair blocking and quasiparticle alignments. However, present calculations remain unable to reliably (i.e., in all cases) reproduce identical bands and it remains to be conclusively shown that the phenomenon of identical bands can be explained with current theoretical techniques. This is clearly a challenge for nuclear structure theory.

ACKNOWLEDGMENTS

This research was supported in part by the U.S. Department of Energy under Contract Nos. DE-AC03-76SF00098 (Lawrence Berkeley National Laboratory), DE-FG02-96ER40963 (University of Tennessee), DE-FG05-87ER40361 (Joint Institute for Heavy Ion Research), and DE-AC05-96OR22464 with Lockheed Martin Energy Research Corp. (Oak Ridge National Laboratory), by the Polish Committee for Scientific Research (KBN) under Contract No. 2 P03B 040 14 and NATA under Grant No. CFG970196.

[1] T. Byrski, F. A. Beck, D. Curien, C. Schuck, P. Fallon, A. Alderson, I. Ali, M. A. Bentely, A. M. Bruce, P. D. Forsyth, D. Howe, J. W. Roberts, J. F. Sharpey-Schafer, G. Smith, and P. J. Twin, Phys. Rev. Lett. **64**, 1650 (1990).
[2] W. Nazarewicz, P. J. Twin, P. Fallon, and J. Garrett, Phys. Rev. Lett. **64**, 1654 (1990).
[3] F. S. Stephens, M. A. Deleplanque, J. E. Draper, R. M. Diamond, C. W. Beausang, W. Korten, W. H. Kelly, F. Azaiez, J. A. Becker, E. A. Henry, N. Roy, M. J. Brinkman, J. A. Cizewski, S. W. Yates, and A. Kuhnert, Phys. Rev. Lett. **64**, 2623 (1990).
[4] F. S. Stephens, M. A. Deleplanque, J. E. Draper, R. M. Diamond, A. O. Macchiavelli, C. W. Beausang, W. Korten, W. H. Kelly, F. Azaiez, J. A. Becker, E. A. Henry, S. W. Yates, M. J. Brinkman, A. Kuhnert, and J. A. Cizewski, Phys. Rev. Lett. **65**, 301 (1990).
[5] C. Baktash, B. Haas, and W. Nazarewicz, Annu. Rev. Nucl. Part. Sci. **45**, 485 (1995).
[6] D. Ye, R. V. F. Janssens, M. P. Carpenter, E. F. Moore, R. R. Chasman, I. Ahmad, K. B. Beard, Ph. Benet, M. W. Drigert, P. B. Fernandez, U. Garg, T. L. Khoo, S. L. Ridley, and F. L. H. Wolfs, Phys. Rev. C **41**, R13 (1990).
[7] M. A. Riley, D. M. Cullen, A. Alderson, I. Ali, T. Bengtsson, M. A. Bentley, A. M. Bruce, P. Fallon, P. D. Forsyth, F. Hanna, S. M. Mullins, W. Nazarewicz, M. Poynter, J. W. Roberts, J. F. Sharpey-Schafer, J. Simpson, G. Sletten, P. J. Twin, R. Wadsworth, and R. Wyss, Nucl. Phys. **A512**, 178 (1990).
[8] G. de France, C. Baktash, B. Hass, and W. Nazarewicz, Phys. Rev. C **53**, R1070 (1996).
[9] C. Shen, Wendong Luo, and Y. S. Chen, Phys. Rev. C **55**, 1792 (1997).
[10] J. A. Becker, N. Roy, E. A. Henry, M. A. Deleplanque, C. W. Beausang, R. M. Diamond, J. E. Draper, F. S. Stephens, J. A. Cizewski, and M. J. Brinkman, Phys. Rev. C **41**, R9 (1990).
[11] J. E. Draper, F. S. Stephens, M. A. Deleplanque, W. Korten, R. M. Diamond, W. H. Kelly, F. Azaiez, A. O. Macchiavelli, C. W. Beausang, E. C. Rubel, J. A. Becker, N. Roy, E. A. Henry, M. J. Brinkman, A. Kuhnert, and S. W. Yates, Phys. Rev. C **42**, R1791 (1990).
[12] C. Schuck, E. Gueorguieva, A. Lopez-Martens, F. Hannachi, A. Korichi, Ch. Vieu, J. S. Dionisio, I. Deloncle, M. Kaci, F. F. Stephens, W. Pohler, B. Schulze, H. Hubel, and R. Wadsworth, Phys. Rev. C **56**, 1667 (1997).
[13] A. Bohr, I. Hamamoto, and B. Mottelson, Phys. Scr. **26**, 267 (1982).
[14] T. L. Khoo, M. P. Carpenter, T. Lauritsen, D. Ackermann, I. Ahmad, D. J. Blumenthal, S. M. Fischer, R. V. F. Janssens, D. Nisius, E. F. Moore, A. Lopez-Martens, T. Dossing, R. Kruecken, S. J. Asztalos, J. A. Becker, L. Bernstein, R. M. Clark, M. A. Deleplanque, R. M. Diamond, P. Fallon, L. P. Farris, F. Hannachi, E. A. Henry, A. Korichi, I. Y. Lee, A. O. Macchiavelli, and F. S. Stephens, Phys. Rev. Lett. **76**, 1583 (1996).
[15] G. Hackman, T. L. Khoo, M. P. Carpenter, T. Lauritsen, A. Lopez-Martens, I. J. Calderin, R. V. F. Janssens, D. Ackermann, I. Ahmad, S. Agarwala, D. J. Blumenthal, S. M. Fisher, D. Nisius, P. Reiter, J. Young, H. Amro, E. F. Moore, F. Hannachi, A. Korichi, I. Y. Lee, A. O. Macchiavelli, T. Dossing, and T. Nakatsukasa, Phys. Rev. Lett. **79**, 4100 (1997).
[16] A. Lopez-Martens, F. Hannachi, A. Korichi, C. Schuck, E. Gueorguieva, Ch. Vieu, B. Haas, R. Lucas, A. Astier, G. Baldsiefen, M. Carpenter, G. de France, R. Duffait, L. Ducroux, Y. Le Coz, Ch. Finck, A. Gorgen, H. Hubel, T. L. Khoo, T. Lauritsen, M. Meyer, D. Prevost, N. Redon, C. Rigollet, H. Savajols, J. F. Sharpey-Schafer, O. Stezowski, Ch. Theisen, U. Van Severen, J. P. Vivien, and A. N. Wilson, Phys. Lett. B **380**, 18 (1996).
[17] K. Hauschild, L. A. Bernstein, J. A. Becker, D. E. Archer, R. W. Bauer, D. P. McNabb, J. A. Cizewski, K.-Y. Ding, W. Younes, R. Krucken, R. M. Diamond, R. M. Clark, P. Fallon, I.-Y. Lee, A. O. Macchiavelli, R. MacLeod, G. J. Schmid, M. A. Deleplanque, F. S. Stephens, and W. H. Kelly, Phys. Rev. C **55**, 2819 (1997).
[18] B. Singh, R. B. Firestone, and S. Y. F. Chu, Report No. LBL-38004, UC-413, 1996.
[19] Y. Liang, M. P. Carpenter, R. V. F. Janssens, I. Ahmad, R. G. Henry, T. L. Khoo, T. Lauritsen, F. Soramel, S. Pilotte, J. M. Lewis, L. L. Riedinger, C.-H. Yu, U. Garg, W. Reviol, and I. G. Bearden, Phys. Rev. C **46**, R2136 (1992).
[20] D. M. Cullen, M. A. Riley, A. Alderson, I. Ali, C. W. Beausang, T. Bengtsson, M. A. Bentley, P. Fallon, P. D. Forsyth, F. Hanna, S. M. Mullins, W. Nazarewicz, R. J. Poynter, P. H. Regan, J. W. Roberts, W. Satuła, J. F. Sharpey-Schafer, J. Simpson, G. Sletten, P. J. Twin, R. Wadsworth, and R. Wyss, Phys. Rev. Lett. **65**, 1547 (1990).
[21] P. Fallon, W. Nazarewicz, M. A. Riley, and R. Wyss, Phys. Lett. B **276**, 427 (1992).
[22] R. Wyss and W. Satuła, Phys. Lett. B **351**, 393 (1995).
[23] S. Fisher, M. P. Carpenter, R. V. F. Janssens, B. Crowell, I. Ahmad, D. J. Blumenthal, T. L. Khoo, T. Lauritsen, and D. Nisius, Phys. Rev. C **53**, 2126 (1996).
[24] W. Satuła, R. Wyss, and P. Magierski, Nucl. Phys. **A578**, 45 (1994).
[25] W. Satuła and R. Wyss, Phys. Rev. C **50**, 2888 (1994).
[26] B. Gall, P. Bonche, J. Dobaczewski, H. Flocard, and P.-H. Heenen, Z. Phys. A **348**, 183 (1994).
[27] J. Terasaki, P.-H. Heenen, P. Bonche, J. Dobaczewski, and H. Flocard, Nucl. Phys. **A593**, 1 (1995).
[28] A. Valor, J. L. Egido, and L. M. Robledo, Phys. Lett. B **392**, 249 (1997).
[29] A. Villafranca and J. L. Egido, Phys. Lett. B **408**, 35 (1997).
[30] R. R. Chasman, Phys. Rev. C **14**, 1935 (1976).
[31] H. J. Lipkin, Ann. Phys. (N.Y.) **9**, 272 (1960).
[32] Y. Nogami, Phys. Rev. B **134**, B313 (1964).
[33] A. Goodfellow and Y. Nogami, Can. J. Phys. **44**, 1321 (1966).
[34] H. C. Pradhan, Y. Nogami, and J. Law, Nucl. Phys. **A201**, 357 (1973).
[35] P. Magierski, S. Ćwiok, J. Dobaczewski, and W. Nazarewicz, Phys. Rev. C **47**, 2418 (1993).
[36] S. Ćwiok, J. Dudek, W. Nazarewicz, J. Skalski, and T. Werner, Comput. Phys. Commun. **46**, 379 (1987).
[37] P. Möller and R. Nix, Nucl. Phys. **A536**, 20 (1992).
[38] H. Sakamoto and T. Kishimoto, Phys. Lett. B **245**, 321 (1990).
[39] V. M. Strutinsky, Yad. Fiz. **3**, 614 (1966) [Sov. J. Nucl. Phys. **3**, 449 (1966)]; Nucl. Phys. **A95**, 420 (1967).
[40] V. M. Strutinsky, Nucl. Phys. **A122**, 1 (1968).
[41] S. Cohen, F. Plasil, and W. J. Swiatecki, Ann. Phys. (N.Y.) **82**, 557 (1974).
[42] W. Satuła and R. Wyss, Phys. Scr. **T56**, 159 (1995).

[43] E. Chabanat, P. Bonche, P. Haensel, J. Meyer, and R. Schaeffer, Nucl. Phys. **A635**, 231 (1998).
[44] C. Rigollet, P. Bonche, H. Flocard, and P.-H. Heenen, Phys. Rev. C **59**, 3120 (1999).
[45] J. Terasaki, H. Flocard, P.-H. Heenen, and P. Bonche, Phys. Rev. C **55**, 1231 (1997).
[46] P.-H. Heenen and R. V. F. Janssens, Phys. Rev. C **57**, 159 (1998).
[47] P. Ring and P. Schuck, *The Nuclear Many-Body Problem* (Springer-Verlag, Berlin, 1980).